Recent Antarctic ice mass loss from radar interferometry and regional climate modelling

ERIC RIGNOT[1,2,3]*, JONATHAN L. BAMBER[4], MICHIEL R. VAN DEN BROEKE[5], CURT DAVIS[6], YONGHONG LI[6], WILLEM JAN VAN DE BERG[5] AND ERIK VAN MEIJGAARD[7]

[1]University of California Irvine, Earth System Science, Irvine, California 92697, USA
[2]Jet Propulsion Laboratory, California Institute of Technology, Pasadena, California 91109, USA
[3]Centro de Estudios Cientificos, Arturo Prat 514, Valdivia, Chile
[4]University of Bristol, Bristol BS8 1SS, UK
[5]Institute for Marine and Atmospheric Research (IMAU), Utrecht University, 3584 CC Utrecht, The Netherlands
[6]University of Missouri-Columbia, Columbia, Missouri 65211, USA
[7]Royal Netherlands Meteorological Institute (KNMI), 3732 GK De Bilt, The Netherlands
*e-mail: erignot@uci.edu

Published online: 13 January 2008; doi:10.1038/ngeo102

Large uncertainties remain in the current and future contribution to sea level rise from Antarctica. Climate warming may increase snowfall in the continent's interior[1–3], but enhance glacier discharge at the coast where warmer air and ocean temperatures erode the buttressing ice shelves[4–11]. Here, we use satellite interferometric synthetic-aperture radar observations from 1992 to 2006 covering 85% of Antarctica's coastline to estimate the total mass flux into the ocean. We compare the mass fluxes from large drainage basin units with interior snow accumulation calculated from a regional atmospheric climate model for 1980 to 2004. In East Antarctica, small glacier losses in Wilkes Land and glacier gains at the mouths of the Filchner and Ross ice shelves combine to a near-zero loss of 4 ± 61 Gt yr^{-1}. In West Antarctica, widespread losses along the Bellingshausen and Amundsen seas increased the ice sheet loss by 59% in 10 years to reach 132 ± 60 Gt yr^{-1} in 2006. In the Peninsula, losses increased by 140% to reach 60 ± 46 Gt yr^{-1} in 2006. Losses are concentrated along narrow channels occupied by outlet glaciers and are caused by ongoing and past glacier acceleration. Changes in glacier flow therefore have a significant, if not dominant impact on ice sheet mass balance.

The mass balance of Antarctica is determined from the difference between two competing processes of ice discharge into the ocean by glaciers and ice streams and accumulation of snowfall in the vast interior, which are two large numbers affected by significant uncertainties[2,12]. Estimates of ice discharge have been sporadic in nature owing to the limited availability of ice velocity and thickness data at the grounding line of Antarctica, as well as precise knowledge of the grounding-line positions. Similarly, estimates of snowfall have been affected by uncertainties associated with the interpolation of sparse *in situ* data of varying quality and temporal coverage over the entire continent.

Here, we present a nearly complete map of surface velocities along the periphery of Antarctica (Fig. 1) obtained from interferometric synthetic-aperture radar (InSAR) data collected between 1992 and 2006 by the European Earth Remote Sensing (ERS-1 and 2), the Canadian Radarsat-1 and the Japanese Advanced Land Observing satellites. Our map covers all major outlet glaciers, ice streams and tributaries of importance for mass flux calculation, with ice velocity ranging from 100 to 3,500 m yr^{-1}, at a precision of 5 to 50 m yr^{-1} (see the Methods section). Short-time variations in velocity, for example, due to ocean tides, are averaged out over the 24 to 46 day repeat period of our measurements. Velocities at the grounding line of fast-moving glaciers are assumed to be depth independent, which introduces errors of much less than 1% (ref. 3).

Using double-difference interferometry, we mapped glacier grounding lines with a precision of 100 m all around Antarctica, except for eight glaciers south of 81° South where we used the Moderate Resolution Imaging Spectroradiometer (MODIS) mosaic[13] with a precision of 1 km. Grounding-line thickness is derived from surface elevation assuming ice to be in hydrostatic equilibrium with sea water (see the Methods section). In selected parts of West Antarctica, we have direct measurements of ice thickness with a precision of 10 m instead (see Supplementary Information, Table S1). For surface elevation, we use a new digital elevation model (DEM) combining precise laser altimeter data from the Ice Cloud and land Elevation Satellite from 2003–2004, ERS-1/2 radar altimeter data from 1994 corrected for temporal changes in between[1,14] and the new GGM02 geoid[15]. Comparison of the DEM with independent laser altimeter data at the grounding line of West Antarctica indicates a vertical precision in elevation of 0.15 ± 4 m. Surface elevation above mean sea level is then converted into solid-ice surface elevation after applying a firn depth correction[16]. We estimate the random error in inferred thickness to range from 80 to 120 m when accounting for uncertainties in grounding-line position, surface elevation, firn depth correction and geoid height. For verification, at the grounding line of Pine Island Bay glaciers, our thickness values are within 14 ± 60 m of direct thickness measurements[10] ranging from 420 to 1,460 m.

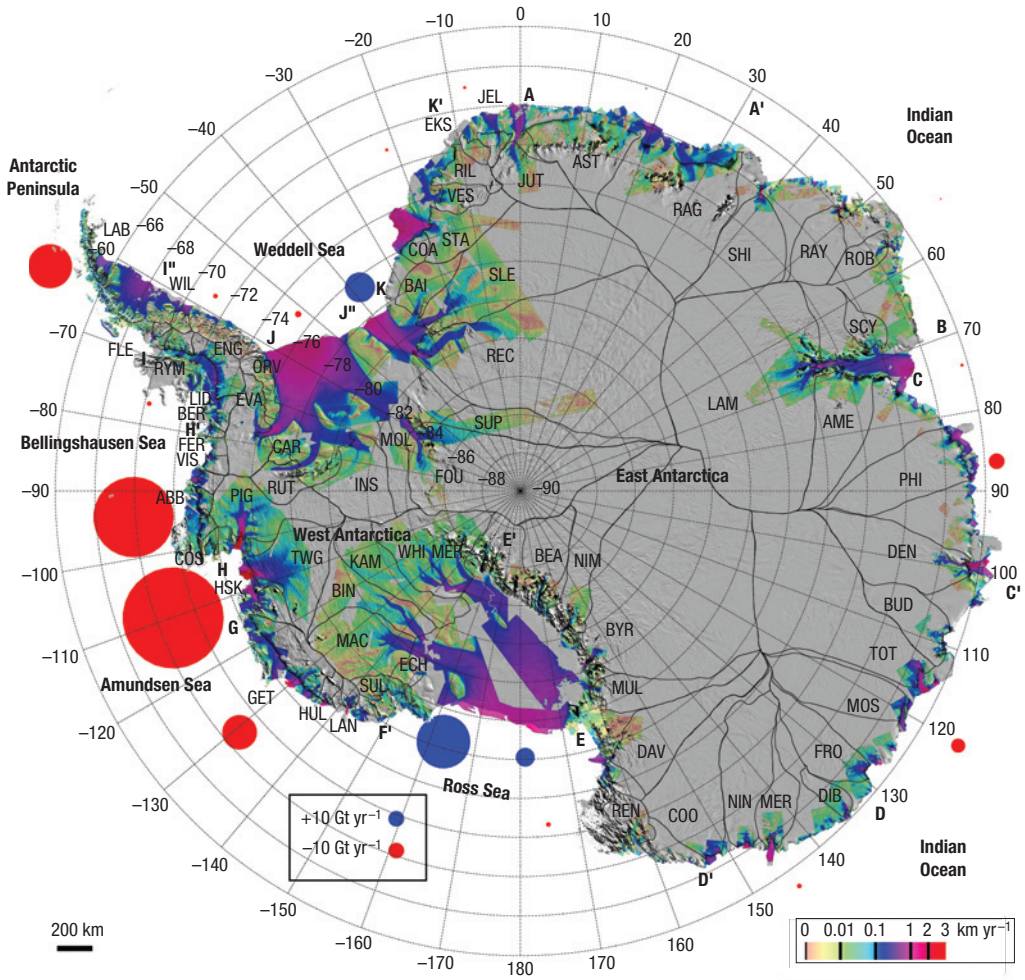

Figure 1 Ice velocity of Antarctica colour coded on a logarithmic scale and overlaid on a MODIS mosaic[13]. Circles denote mass loss (red) or gain (blue) of large basins in gigatonnes per year. Drainage basins are black lines extending from the grounding-line flux gates. Letters A–K′ indicate large basins[20]. Ice velocities for Siple Coast ice streams and Ronne Ice Shelf are from refs 22,23. See Supplementary Information for acronyms and the Methods section for velocity precision.

Solid-ice fluxes are then calculated combining vector ice velocity and ice thickness, with a precision that is glacier dependent and ranges from 2 to 15% (see the Supplementary Information). The end points of the selected flux gates define the extent of the glacier drainage basins determined from the DEM. Individual drainage basins are grouped into large units labelled A to K′.

Snowfall accumulation is from the RACMO2/ANT regional atmospheric climate model, at 55 km resolution, averaged for 1980–2004 (refs 17–19). Lateral forcings are taken from European Center for Medium-Range Weather Forecasting reanalyses (ERA-40) for the period 1980–2002, supplemented with European Center for Medium-Range Weather Forecasting operational analyses after August 2002. Comparisons with 1,900 independent field data show excellent agreement ($R = 0.82$) with the model[18]. The model predicts higher coastal precipitation and wetter conditions in West Antarctica and the western Peninsula[17] than older maps obtained by interpolating limited field data using meteorological variables[20] or satellite passive microwave data[21]. Few reliable *in situ* coastal accumulation data exist for comparison, but in the high-accumulation sector of the Getz Ice Shelf (basin F′G), the model predicts precipitation levels consistent with a 2,030 mm yr^{-1} record at Russkaya station (74°46′ S, 136°52′ W) for 1981–1989. Older maps yield accumulation levels 3 times lower, which imply a local mass balance 20 times more negative and high rates of glacier thinning that are not observed[2]. The RACMO2/ANT accumulation values yield comparable losses for Pine Island and Thwaites glaciers, which is consistent with the similarity of their thinning rates[2]; other maps yield twice more thinning for Thwaites. Finally, the model does not mix data from different time periods and fully incorporates temporal changes in snowfall between 1980 and 2004. A statistical analysis of absolute errors (see the Methods section) yields an uncertainty in accumulation varying from 10% in dry, large basins to 30% in wet, small coastal basins.

Ice flux and snowfall are compared for each glacier, for large basins A–K′, and for the Peninsula, East and West Antarctica. To include non-surveyed areas, we apply a scaling factor on the mass fluxes of each large basin A–K′ based on the percentage surveyed area versus total area to cover 100% of Antarctica (Table 1). In East Antarctica, we obtain a near-zero mass balance of -4 ± 61 Gt yr^{-1}. The J″K Filchner[22] and E′E Ross sectors are gaining mass, but this is compensated by the mass loss in Wilkes Land (basin CE) from the Philippi, Denman, Totten, Moscow University Ice Shelf, Cook Ice Shelf and David glaciers. Interestingly, all of these glaciers are marine based, that is, grounded well below sea level[2], and therefore

Table 1 Mass balance of Antarctica in gigatonnes (10^{12} kg) per year by sector for the year 2000. Area: area surveyed. Input: snow accumulation $\pm\sigma$ of surveyed area. Outflow: grounding-line ice flux $\pm\sigma$ of surveyed area. Net: mass balance calculated as Input minus Outflow, $\pm\sigma$. Net+: mass balance scaled on the basis of total area (Area+) versus area surveyed (Area), except for basin II″ where we use refs 8,9. Input+: total snowfall in Area+ $\pm\sigma$. Mass losses for 1996 and 2006 differ from those in the year 2000 in basins GH and II″ (see Table 2).

Sector	Area (10^3 km^2)	Input (Gt yr^{-1})	Outflow (Gt yr^{-1})	Net (Gt yr^{-1})	Net+ (Gt yr^{-1})	Area+ (10^3 km^2)	Input+ (Gt yr^{-1})
J″K Filchner	1,698	93±8	75±4	18±9	19±10	1,780	100±9
KK′ Riiser Larsen	218	42±8	45±4	−3±9	−3±11	246	50±10
K′A Jutulstraumen	159	26±7	28±2	−1±8	−1±9	178	32±9
AA′ Queen Maud Land	615	60±9	60±7	0±11	0±12	622	62±9
A′B Enderby Land	354	39±5	40±2	−1±5	−1±9	645	115±14
BC Lambert	1,197	73±10	77±4	−4±11	−4±12	1,332	87±12
CC′ Philippi, Denman	434	81±13	87±7	−7±15	−11±24	702	137±22
C′D Totten, Frost	1,053	198±37	207±13	−8±39	−9±43	1,162	261±49
DD′ Cook, Mertz, Ninnis	563	92±14	94±6	−2±16	−2±19	691	136±21
D′E Victoria Land	267	20±1	22±3	−2±4	−3±6	450	62±4
EE′ TransAntarctic	1,441	61±10	49±4	11±11	13±13	1,639	89±15
East Antarctica 2000	7,998	786±48	785±20	1±52	−4±61	9,447	1,131±69
E′F′ Siple Coast	751	110±7	80±2	31±7	34±8	845	130±8
F′G Getz, Hull, Land	119	108±28	128±18	−19±33	−23±39	140	128±33
GH Pine Is., Thwaites	393	177±25	237±4	−61±26	−64±27	417	196±28
HH′ Ferrigno, Abbot	55	51±16	86±10	−35±19	−49±27	78	71±22
JJ″ Ronne	933	142±11	145±7	−4±13	−4±14	1,028	165±13
West Antarctica 2000	2,251	588±49	676±22	−88±54	−106±60	2,508	690±57
H′I English Coast	92	71±21	78±7	−7±23	−7±24	98	77±23
II″ Graham Land	13	15±5	20±3	−5±6	−15±8	78	125±46
I″J East Palmer Land	11	8±4	9±2	−1±4	−6±18	52	32±14
Antarctic Peninsula 2000	116	94±21	107±8	−13±23	−28±45	228	234±53
Antarctica 2000	10,365	1,469±87	1,568±31	−100±78	−138±92	12,183	2,055±122

more prone to instabilities. In West Antarctica, the well-known mass gain of the E′F′ Siple Coast basin[23] is small compared with the combined mass loss from the F′G, GH and HH′ basins, which include the entire Amundsen and Bellingshausen sea coasts, and not just Pine Island Bay. The mass loss inferred from F′H′ is much larger than in a previous survey[12] that did not include many high-loss, small glaciers in the GF′ and HH′ basins and ongoing glacier acceleration in basin GH. Overall, the West Antarctic ice sheet lost 106±60 Gt yr^{-1} in the year 2000.

In the Antarctic Peninsula, the H′I and I″J basins of Palmer Land are near balance, despite a reported increase in snowfall[17], but basin II″ of Graham Land is out of balance. On the east coast, the Larsen A and B glaciers experienced an abrupt acceleration (300% on average) in 2002, which increased their mass loss from 3±1 in 1996 and 2000, to 31±9 Gt yr^{-1} in 2006 (ref. 11). Farther south, airborne laser altimetry data suggest that the Larsen C glaciers are close to balance[6]. But on the west coast, the glaciers have experienced widespread ice-front retreat, enhanced melt and continuous speed up[9]. We have no thickness data for these glaciers, and there is no floating section. A 12% speed up in 10 years, enhanced melt and a net accumulation of 42±14 Gt yr^{-1} suggest a loss of 7±4 Gt yr^{-1} in 1996, 10±5 Gt yr^{-1} in 2000 and 13±7 Gt yr^{-1} in 2006. The combined loss for the Peninsula then becomes 25±45 Gt yr^{-1} in 1996, increasing by 140% in 2006 to 60±46 Gt yr^{-1} (Table 2).

Changes in surface elevation in basin F′H′ for 1995–2005 (Fig. 2) reveal broad-scale, centimetre-level variations in snowfall in the interior (wetter conditions in H′H, and drier in F′E′ (ref. 17)), but pronounced, metre-scale thinning concentrated in narrow channels occupied by outlet glaciers and extending in the flow direction across the entire coastal range. The strong, widespread correlation between ice thinning and ice velocity (>50 m yr^{-1}), for example, on the Berg, Ferrigno, Venable, Pine Island, Thwaites, Smith and Getz glaciers, indicates that thinning is caused by the velocity of glaciers being well above that required to maintain mass balance, that is, ice stretches longitudinally, which causes it to thin vertically. In basin GH, we find that Pine Island Glacier accelerated 34% in 1996–2006, Smith 75%, Pope 20%, Haynes 27% and Thwaites is widening[11]. The mass flux from basin GH thereby increased 21% since 1996 and the mass loss doubled from 41±27 Gt yr^{-1} in 1996 to 64±27 Gt yr^{-1} in 2000 and 90±27 Gt yr^{-1} in 2006 (Table 2). This is the largest loss in Antarctica. In contrast, we detect no glacier acceleration in basins

Table 2 Mass balance in gigatonnes (10^{12} kg) per year for 1996 and 2006 of basins II″ and G H, West Antarctica, the Peninsula and the entire Antarctic ice sheet.

Sector	Outflow (Gt yr^{-1})	Net (Gt yr^{-1})	Net+ (Gt yr^{-1})
GH Pine Is. Thwaites 1996	215±3	−39±25	−41±27
GH Pine Is. Thwaites 2006	261±4	−85±26	−90±27
West Antarctica 1996	654±22	−66±53	−83±59
West Antarctica 2006	700±23	−112±54	−132±60
II″ Graham Land 1996	20±3	−5±6	−12±7
II″ Graham Land 2006	49±3	−34±6	−47±9
Peninsula 1996	107±8	−13±23	−25±45
Peninsula 2006	136±10	−42±24	−60±46
Antarctica 1996	1,546±30	−78±78	−112±91
Antarctica 2006	1,621±32	−153±78	−196±92

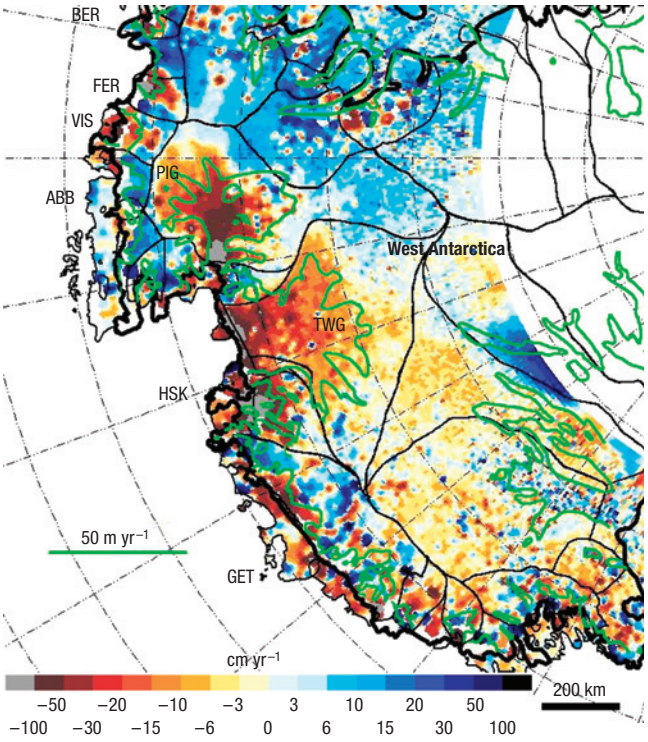

Figure 2 Changes in surface elevation (centimetres per year) for basin F′H′. Values were derived from ERS-2 and Envisat radar altimeter data for 1995–2005 and colour coded from red (thinning) to blue (thickening), overlaid on 50 m yr^{-1} velocity contours in green. Areas of fast flow in F′H′ correspond to areas of concentrated thinning, in contrast with other glaciers.

HH′ and GF′ in 1992–2006, which implies that these glaciers must have accelerated out of equilibrium well before 1992 and maintained high speeds since then. This is exactly what happened to Fleming Glacier following the demise of Wordie Ice Shelf[8]. Similarly, in basin CE″ in East Antarctica, ice thinning is detected along the trenches of the David, Cook, Frost, Moscow University, Totten and Denman glaciers[2], yet we find no change in speed of these glaciers between 1996 and 2006, and not even a change in speed since 1957 on Denman Glacier[11]. Glacier acceleration out of equilibrium must have preceded our period of observation there as well, and the glaciers must have been steadily out of balance for many decades, not just the recent past.

Glaciers that flow into large ice shelves (basins JK, F′E, BC) are near balance or thickening. This is consistent with their stabilization by buttressing and their distance to ocean heat sources associated with the Antarctic Circumpolar Current[22]. Mass losses in the Amundsen Sea and the northern Peninsula are caused by ongoing acceleration, not by a change in snowfall because snowfall increased in 1980–2004, especially in the Peninsula[17]. Fast flow is explained by the ungrounding of glaciers owing to the thinning or collapse of their buttressing ice shelves[6] or to a reduction in backforce resistance at the ice front as glacier fronts thin because of warmer air or warmer ocean temperatures[4,9]. In the Amundsen Sea and the western Peninsula, ice-shelf melting is fuelled by intrusions of warm circumpolar deep water (CDW) onto the continental shelf down deep troughs carved into the sea floor during past ice ages[24,25]. In East Antarctica, there is no report of CDW intrusion in Wilkes Land. A southward migration of the Antarctic Circumpolar Current[26] caused by an increasingly positive southern annular mode may have, in favourable conditions[24], entrained overspills of CDW onto the continental shelf and trigger glacier acceleration, but this hypothesis cannot be confirmed at present.

Our results provide a nearly complete assessment of the spatial pattern in mass flux and mass change along the coast of Antarctica, glacier by glacier, with lower error bounds than in previous incomplete surveys, and a delineation of areas of changes versus areas of near stability. Over the time period of our survey, the ice sheet as a whole was certainly losing mass, and the mass loss increased by 75% in 10 years. Most of the mass loss is from Pine Island Bay sector of West Antarctica and the northern tip of the Peninsula where it is driven by ongoing, pronounced glacier acceleration. In East Antarctica, the loss is near zero, but the thinning of its potentially unstable marine sectors calls for attention. In contrast to major increases in ice discharge, snowfall integrated over Antarctica did not change in 1980–2004 (ref. 27) and even slightly increased in areas of large loss[17]. We conclude that the Antarctic ice sheet mass budget is more complex than indicated by the temporal evolution of its surface mass balance. Changes in glacier dynamics are significant and may in fact dominate the ice sheet mass budget.

METHODS

FIRN DEPTH CORRECTION

Ice thickness, H, is deduced from surface elevation above mean sea level with reference to the GGM02 geoid[15], h, as $H = (h - \Delta H)\rho_{sea}/(\rho_{sea} - \rho_{ice})$, where the density of sea water, $\rho_{sea} = 1{,}028\,\mathrm{kg\,m^{-3}}$ (at 34 p.s.u. salinity, 1 km depth), the density of solid ice, $\rho_{ice} = 917\,\mathrm{kg\,m^{-3}}$ and ΔH is the firn depth correction. For $H = 1$ km, a 4 m uncertainty in ΔH introduces a 4% uncertainty in thickness and flux. Earlier work assumed a constant firn depth correction. We calculate ΔH from a firn densification model[16] driven by surface density using 25-year-average air temperature, snow accumulation and wind speed from RACMO2/ANT. ΔH varies from 0 to 20 m. Its precision is 2–3 m on the basis of a comparison with firn core data at the critical densities of 550 and 880 kg m^{-3}.

SNOW ACCUMULATION ERROR

Snow accumulation is the arithmetic average of the values given in refs 18,19. We use 1,900 *in situ* independent observations, SMB_o, to calculate absolute errors. The error for the observations is modelled as $E_o = 5 + 0.15\ SMB_o$ in kg m^{-2} yr^{-1} where the second term accounts for the uncertainty associated with spatial variability. The error for the modelled values, SMB_m, is modelled as $E_m = 9 + 0.10\ SMB_m + 0.00033\ SMB_m^2$ in kg m^{-2} yr^{-1}. This representation reflects that the model is well calibrated with many good observations for low and medium values, but that the relative and absolute errors increase for high values where few reliable observations exist. The relative error is maximized at 30% for $SMB_m > 557\,\mathrm{kg\,m^{-2}\,yr^{-1}}$. Coefficients for the modelling of E_m were optimally chosen by examining the distribution of differences, $SMB_m - SMB_o$, normalized by the total error margin, that is, the squared sum of E_o and E_m. With our selection of coefficients, we obtain a normal distribution with $\sigma = 1$, which provides strong statistical support for the error analysis. To calculate accumulation uncertainty at the basin scale, we also account for the spatial autocorrelation of errors. The correlation length of $(SMB_m - SMB_o)$ varies from 161 km below 2,000 m elevation to 300 km above 2,000 m. Combining these correlation lengths with the error modelling, we obtain total errors in AK′ basins (Table 1) ranging from 10% in large, dry basins to 30% in wet and smaller coastal basins. These errors represent our most likely estimate of absolute errors, not the 95% confidence interval. Previous attempts at defining accumulation errors only addressed interpolation errors.

VELOCITY AND MASS FLUX ERRORS

Ice velocity is measured with speckle tracking on Radarsat-1 24 day, Japanese Advanced Land Observing PALSAR 46 day (basin GF′) and ERS-1 9 day (basin H′I) repeats, and interferometrically using ascending/descending ERS-1/2 tandem pairs (basin HG) with an ERS-1/2 precision of 2–5 m yr^{-1}; and with a combination of interferometric phase and speckle tracking (basin D′C′), with a precision of 20–50 m yr^{-1}. Systematic errors are negligible compared with random errors because we use stagnant areas for calibration and combine multiple tracks with different look directions. The unknown positive bias between surface and vertically integrated velocity is much less than 1%.

Systematic errors in thickness are less than 1%, whereas random errors range from 10 to 120 m (see Supplementary Information, Table S1). The percentage error in mass flux is calculated as the sum of the percentage error in velocity and the percentage error in thickness. This is appropriate for plug flow or U-shaped velocity profiles, which is the case for most large Antarctic glaciers. For glaciers that approach a V-shaped velocity profile, our errors may be underestimated by a factor of 2. Errors in Table 1 and Supplementary Information, Table S1 are only random errors. Systematic errors are not known but small, so that actual errors may be slightly higher. Decadal changes in velocity were only available for glaciers mentioned in the text, ref. 11 or Table 2, and were assumed to be zero elsewhere.

Received 29 August 2007; accepted 27 November 2007; published 13 January 2008.

References

1. Davis, C. H., Li, Y., McConnell, J. R., Frey, M. M. & Hanna, E. Snowfall-driven growth in East Antarctic Ice Sheet mitigates recent sea level rise. *Science* **308**, 1898–901 (2005).
2. Shepherd, A. & Wingham, D. Recent sea-level contributions of the Antarctic and Greenland Ice Sheets. *Science* **315**, 1529–1532 (2007).
3. Huybrechts, P., Gregory, J., Janssens, I. & Wild, M. Modelling Antarctic and Greenland volume changes during the 20th and 21st centuries forced by GCM time slice integrations. *Global Planet. Change* **42**, 83–105 (2004).
4. Thomas, R. H., Rignot, E. & Kanagaratnam, P. Force-perturbation analysis of Pine Island Glacier, Antarctica, suggests cause for recent acceleration. *Ann. Glaciol.* **39**, 133–138 (2004).
5. Scambos, T., Bohlander, J. A., Shuman, C. A. & Skvarca, P. Glacier acceleration and thinning after ice shelf collapse in the Larsen B embayment, Antarctica. *Geophys. Res. Lett.* **31**, L18402 (2004).
6. Rignot, E. *et al.* Accelerated ice discharge from the Antarctic Peninsula following the collapse of Larsen B ice shelf. *Geophys. Res. Lett.* **31**, L18401 (2004).
7. De Angelis, H. & Skvarca, P. Glacier surge after ice shelf collapse. *Science* **299**, 1560–1562 (2003).
8. Rignot, E. *et al.* Recent ice loss from the Fleming and other glaciers, Wordie Bay, West Antarctic Peninsula. *Geophys. Res. Lett.* **32**, L07502 (2005).
9. Pritchard, H. & Vaughan, D. Widespread acceleration of tidewater glaciers on the Antarctic Peninsula. *J. Geophys. Res.* **112** (2007) (doi:10.1029/2006JF000597).
10. Thomas, R. H. *et al.* Accelerated sea-level rise from West Antarctica. *Science* **306**, 255–258 (2004).
11. Rignot, E. Changes in ice dynamics and mass balance of the Antarctic ice sheet. *Phil. Trans. R. Soc. A* **364**, 1637–1656 (2006).
12. Rignot, E. & Thomas, R. H. Mass balance of polar ice sheets. *Science* **297**, 1502 (2002).
13. Haran, T., Bohlander, J., Scambos, T. & Fahnestock, M. *MODIS Mosaic of Antarctica (MOA) Image Map* (National Snow and Ice Data Center, Boulder, 2005).
14. Bamber, J. L. & Gomez, J. L. The accuracy of digital elevation models of the Antarctic continent. *Earth Planet. Sci. Lett.* **237**, 516–523 (2005).
15. Tapley, B. *et al.* GGM02—An improved Earth gravity field model from GRACE. *J. Geodesy* (2005) (doi:10.1007/s00190-005-0480-z).
16. van den Broeke, M. R. Towards quantifying the contribution of the Antarctic ice sheet to global sea level change. *J. Phys. IV France* **139**, 179–187 (2006).
17. van den Broeke, M., van de Berg, W. & van Meijgaard, E. Snowfall in coastal West Antarctica much greater than previously assumed. *Geophys. Res. Lett.* **33**, L02505 (2006).
18. van de Berg, W., van den Broeke, M., Reijmer, C. & van Meijgaard, E. Reassessment of the Antarctic surface mass balance using calibrated output of a regional atmospheric climate model. *J. Geophys. Res.* **111**, D11104 (2006).
19. van den Broeke, M., van de Berg, W. J., van Meijgaard, E. & Reijmer, C. Identification of Antarctic ablation areas using a regional atmospheric climate model. *J. Geophys. Res.* **111**, D18110 (2006).
20. Giovinetto, M. & Zwally, J. Spatial distribution of net surface accumulation on the Antarctic ice sheet. *Ann. Glaciol.* **31**, 171 (2000).
21. Arthern, R. J., Winebrenner, D. P. & Vaughan, D. G. Antarctic snow accumulation mapped using polarization of 4.3-cm wavelength microwave emission. *J. Geophys. Res.* **111**, D06107 (2006).
22. Joughin, I. & Bamber, J. Thickening of the ice stream catchments feeding the Filchner-Ronne ice shelf, Antarctica. *Geophys. Res. Lett.* **32**, L17503 (2005).
23. Joughin, I. & Tulaczyk, S. Positive mass balance of the Ross Ice Streams, West Antarctica. *Science* **295**, 476–480 (2002).
24. Jacobs, S. Observations of change in the Southern Ocean. *Phil. Trans. R. Soc. A* **364**, 1657–1681 (2006).
25. Domack, E. W., Burnett, A. & Leventer, A. *Antarctic Research Series Volume 79: Peninsula and Climate Variability* 1–14 (American Geophysical Union, Washington DC, 2003).
26. Gille, S. Warming of the southern ocean since the 1950s. *Science* **295**, 1275–1277 (2002).
27. Monaghan, A. J. *et al.* Insignificant change in Antarctic snowfall since the international geophysical year. *Science* **313**, 827–831 (2006).

Acknowledgements

We thank R. Arthern for discussions. This work was carried out at Caltech's Jet Propulsion Laboratory, the University of California Irvine and the University of Missouri, Columbia, under a contract with NASA's Cryospheric Science Program. J.L.B. was supported by NERC grant NE/E004032/1. SAR data were provided by the European Space Agency VECTRA project, the Canadian Space Agency, the Japanese Space Agency, and the Alaska Satellite Facility. ERS-2 radar altimeter data were provided by NASA/GSFC.

Correspondence and requests for materials should be addressed to E.R.

Supplementary Information accompanies this paper on www.nature.com/naturegeoscience.

Author contributions

All authors discussed the results and commented on the manuscript. E.R. led the remote sensing analysis, development of the paper and integration of the results, J.L.B. provided a digital elevation model and analysed its accuracy, M.R.B., W.J.B. and E.M. contributed calculations of snow accumulation, firn depth correction and associated errors and C.D. and Y.L. analysed elevation changes from satellite radar altimeter data.

Supplementary Material

Table S1: Glacier mass budget organized by basins A to K' as in ref. 20. Sectors corresponding to unnamed glaciers were named after a bay or an ice shelf. Area, drainage basin in million square km. A, snow accumulation in Gigatons of water per year (Gt/yr). F, solid ice flux in Gt/yr and uncertainty in flux σ calculated from the error in ice velocity, δV, ice thickness, δH, the center ice thickness, H, and the velocity, V as, $\sigma / F = \delta H/H + \delta V/V$. ΔH, firn depth correction in m (ISR indicates ice sounding radar thickness instead). Mass balance is A minus F. Year, year of velocity data. GL, grounding line determined from InSAR or MOA[13]. Ice fluxes for F'E are from ref. 23. Ice thickness for SUL (ref. S1), for FLE, PIG, TWG, HSK[10], and BEDMAP for SUF.

LAB = Larsen A and B glaciers[6]. FLE =Fleming and other glaciers[8]. RYM, ENG = Rymill and English coasts. LID = Lidke and other glaciers. BER, FER = Berg and Ferrigno ice streams. VIS, ABB, COS, GET, SUL = Glaciers flowing into Venable, Abbot, Cosgrove, Getz and Sulzberger ice shelves. PIG, TWG, HSK, HUL, LAN = Pine Island, Thwaites, Haynes, Pope, Smith, Kohler, Hull and Land glaciers. MER, WHI, KAM, BIN, MAC, ECH = Mercer, Whillans, Kamb, Bindschadler, MacAyeal and Echelmeyer ice streams. BEA, NIM, BYR, MUL, DAV, REN = Beardmore, Nimrod, Byrd, Mullock, David and Rennick glaciers. COO, MOS = Glaciers flowing into Cook and Moscow University ice shelves. NIN, MER, DIB, FRO, TOT, DEN, PHI, LAM, SCY = Ninnis, Mertz, Dibble, Frost, Totten, Denman, Philippi and others, Lambert and others, and Scylla and other glaciers. BUD, RAG, AST = Budd, Princess Ragnhild and Princess Astrid coasts. AME = American Highland glaciers. ROB, RAY, SHI = Robert, Rayner and Thyer, Shirase glaciers. JUT = Jutulstraumen. JEL, EKS, RIL = Glaciers flowing into Jelbart, Ekstrom, and Riiser-Larsen ice shelves. VES, STA = Veststraumen, Stancomb-Wills glaciers. COA = Coats Land. BAI, SLE, REC, FOU, MOL, INS, RUT, EVA = Bailey, Slessor, Recovery, Foundation, Moller, Institute, Rutford, Evans ice streams. CAR = Carlson Inlet. ORV, WIL = Orville and Wilkins coasts.

Flux gates are wider than in ref. 12 because of the availability of additional ice velocity and thickness data across larger sectors of ice.

Supplementary References

S1. B. Luyendyk, D. Wilson, *Surface elevation and ice thickness, Western Marie Byrd Land, Antarctica*, Boulder, CO, USA: National Snow and Ice Data Center (2003).

Basin		Area	A	F	σ	V	H	δV	δH	ΔH	A - F	Year	GL
		Mkm^2	Gt/yr	Gt/yr		km/yr	km			m	Gt/yr		
I"J	**WIL**	11	8.1	9.4	2	0.4	0.6	20	80	16	-1	2000	InSAR
II"	**LAB**	6	11.0	36.1	8	2.0	0.6	20	120	12	-25	2004	InSAR
II"	**FLE**	7	3.7	6.2	0	2.0	0.4	10	10	ISR	-3	2000	ISR
H'I	**RYM**	17	10.6	12.9	2	0.4	0.8	20	80	6	-2	1994	InSAR
H'I	**ENG**	54	39.2	31.6	5	0.4	0.9	20	100	15	8	1996	InSAR
H'I	**LID**	17	16.0	23.3	5	0.4	0.8	50	80	17	-7	1996	InSAR
H'I	**BER**	5	5.5	10.1	1	1.2	1.2	50	120	18	-5	1996	InSAR
Peninsula		**116**	**94**	**130**	**11**						**-36**		
HH'	**FER**	14	12.7	25.8	3	1.7	1.5	50	120	18	-13	1992	InSAR
HH'	**VEN**	14	13.4	21.0	3	0.6	1.0	50	80	17	-8	1996	InSAR
HH'	**ABO**	19	18.7	31.7	9	0.3	0.8	50	80	17	-14	1992	InSAR
HH'	**COS**	9	6.3	7.5	3	0.2	1.5	50	80	16	-1	1992	InSAR
GH	**PIG**	164	61.3	84.9	1	2.5	1.1	20	10	ISR	-24	2000	ISR
GH	**THW**	182	75.0	97.1	2	2.0	1.1	20	10	ISR	-22	2000	ISR
GH	**INT**	11	8.9	7.9	0	0.5	1.0	20	10	ISR	1	1996	ISR
GH	**HSK**	37	31.4	47.2	3	0.8	1.5	50	10	ISR	-16	2000	ISR
F'G	**GET**	92	85.8	97.8	18	0.5	0.9	50	80	19	-11	1996	InSAR
F'G	**HUL**	14	12.7	15.8	2	1.1	1.7	50	80	19	-4	1996	InSAR
F'G	**LAN**	13	9.9	14.2	2	1.0	1.3	50	80	18	-4	1996	InSAR
E'F'	**SUL**	34	14.3	7.8	0	0.3	0.9	10	10	ISR	7	2000	ISR
E'F'	**WHI**	232	35.1	30.3	1	0.5	0.6	10	10	ISR	5	1997	ISR
E'F'	**KAM**	153	18.3	0.5	0	0.0	0.6	10	10	ISR	18	1997	ISR
E'F'	**BIN**	140	16.9	15.3	1	0.3	0.6	10	10	ISR	2	1997	ISR
E'F'	**MAC**	175	22.3	24.4	1	0.3	0.6	10	10	ISR	-2	1997	ISR
E'F'	**ECH**	17	3.4	1.5	0	0.3	0.6	10	10	ISR	2	1997	ISR
JJ"	**ORV**	36	11.0	11.6	3	0.1	0.6	10	80	16	0	2000	InSAR
JJ"	**EVA**	109	44.4	44.0	4	0.6	1.5	20	80	19	0	1996	InSAR
JJ"	**CAR**	9	3.6	0.5	1	0.1	1.8	25	80	22	1	1992	InSAR
JJ"	**RUT**	53	18.5	19.1	3	0.4	2.0	50	80	20	0	1992	InSAR
JJ"	**INS**	149	21.9	25.6	3	0.4	1.3	20	80	19	-3	1997	Moa
JJ"	**MOL**	62	7.4	6.5	1	0.1	1.1	10	80	19	1	1997	Moa
JJ"	**FOU**	515	35.0	38.1	3	0.6	2.3	20	80	14	-1	1997	Moa
West		**2251**	**588**	**676**	**22**						**-88**		
J"K	**SUP**	133	7.0	3.9	1	0.1	1.6	20	80	ISR	3	1997	ISR
J"K	**REC**	996	48.6	39.2	3	0.8	1.8	20	80	15	9	1997	Moa
J"K	**SLE**	499	30.6	26.1	3	0.5	1.3	20	80	16	5	1997	InSAR
J"K	**BAI**	71	6.6	5.9	1	0.2	2.0	20	80	17	1	1997	InSAR
D'E	**DAV**	214	10.8	14.6	2	0.5	2.7	50	100	14	-4	1996	InSAR
D'E	**REN**	53	9.4	7.4	3	0.2	1.5	50	100	14	2	2000	InSAR
DD'	**COO**	243	32.2	37.0	5	1.8	1.0	50	100	17	-5	2000	InSAR
DD'	**NIN**	205	25.1	25.3	3	0.8	1.5	50	100	17	0	1996	InSAR
DD'	**MER**	82	19.9	18.5	2	0.8	1.8	50	100	17	1	1996	InSAR
DD'	**DIB**	33	15.1	13.8	2	0.8	1.5	50	100	17	1	1996	InSAR
C'D	**FRO**	136	32.6	36.1	3	1.7	2.0	50	100	16	-4	1996	InSAR
C'D	**HOL**	49	24.5	20.6	2	1.5	2.0	50	100	16	4	1996	InSAR
C'D	**MOS**	181	35.9	41.1	7	0.4	2.5	50	100	16	-6	1996	InSAR
C'D	**TOT**	570	67.9	73.6	8	0.8	2.0	50	100	17	-6	1996	InSAR
C'D	**BUD**	117	37.5	35.3	7	0.5	1.0	50	100	13	3	1996	InSAR
CC'	**DEN**	226	40.7	43.6	3	1.5	2.5	50	100	14	-3	1996	InSAR
CC'	**PHI**	208	40.0	43.7	6	0.5	0.8	20	80	14	-3	2000	InSAR
BC	**LAM**	957	55.8	56.7	3	0.7	3.0	20	100	13	1	1996	InSAR
BC	**SCY**	42	6.4	8.5	2	0.2	1.6	20	80	12	-2	2000	InSAR
BC	**AME**	198	11.3	12.3	2	0.3	1.2	20	80	11	-1	2000	InSAR
A'B	**ROB**	51	10.8	8.0	1	0.8	1.7	20	80	18	3	2000	InSAR
A'B	**RAY**	104	14.2	10.7	1	1.0	1.0	20	80	12	3	2000	InSAR
A'B	**SHI**	199	14.3	21.1	1	2.2	1.3	20	80	15	-7	1996	InSAR
AA'	**QML**	615	59.9	60.1	7	0.2	0.7	20	80	13	1	2000	InSAR
K'A	**JUT**	123	14.1	14.2	1	0.7	2.0	20	80	15	0	1994	InSAR
K'A	**JEL**	19	8.6	9.6	1	0.3	1.0	20	80	16	-1	2000	InSAR
K'A	**EKS**	17	3.8	3.9	1	0.1	0.9	20	80	16	0	2000	InSAR
KK'	**RIL**	51	9.3	11.1	3	0.1	0.7	20	80	15	-1	2000	InSAR
KK'	**VES**	39	8.1	7.7	1	0.2	1.2	20	80	14	0	1996	InSAR
KK'	**STA**	108	16.3	17.5	2	0.7	1.4	20	80	17	-1	1996	InSAR
KK'	**COA**	19	8.2	8.3	2	0.2	0.8	20	80	17	0	2000	InSAR
E E'	**BYR**	997	39.1	30.4	4	0.8	2.0	20	200	12	8	1997	Moa
E E'	**MUL**	119	6.1	5.7	1	0.4	1.0	20	80	13	0	1997	Moa
E E'	**BEA**	102	5.7	6.3	1	0.3	1.3	20	80	13	-1	1997	Moa
E E'	**NIM**	222	9.9	6.9	1	0.4	2.4	20	100	6	3	1997	Moa
East		**7998**	**786**	**785**	**20**						**1**		